Theoretical and Numerical Explorations in Helical and Fan-Beam Tomography

Adel Faridani

Joint work with **Ryan Hass** and **Donald C. Solmon**.

Department of Mathematics

Oregon State University

January 31, 2008

3D Helical Tomography

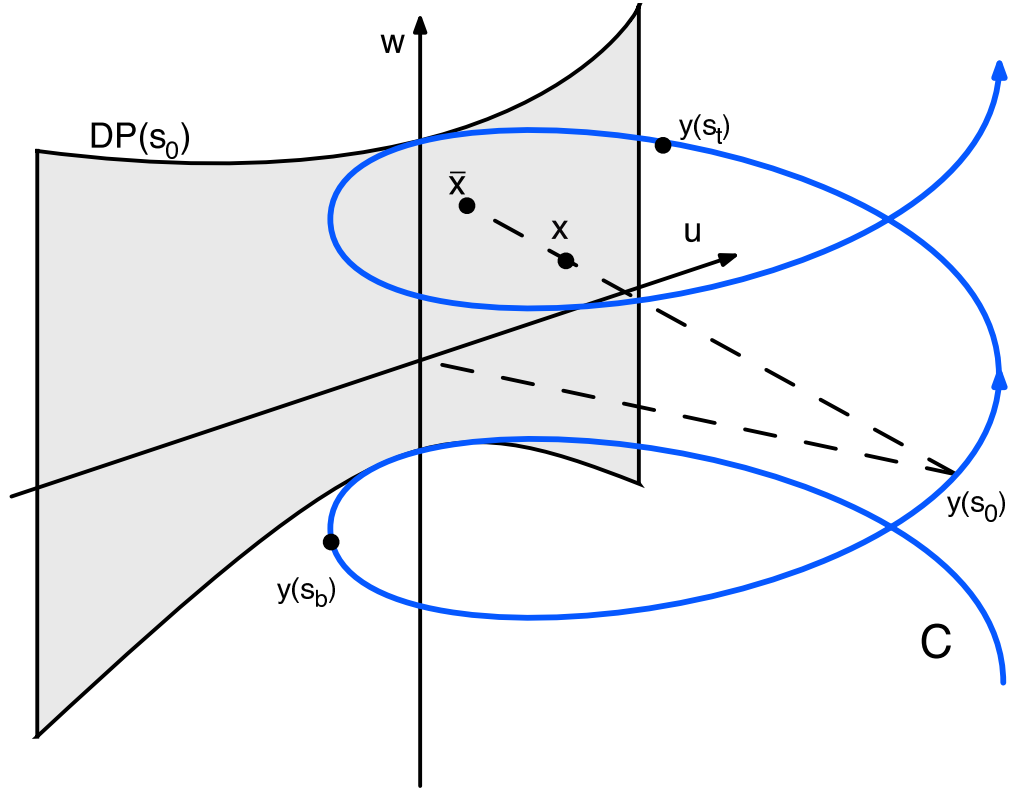

Object contained in a cylinder inside the helix.

Source Curve: $\mathbf{y}(s) = \left[R\,\cos(s),\ R\,\sin(s),\ \dfrac{P}{2\pi}s\right]$

3D Helical Tomography

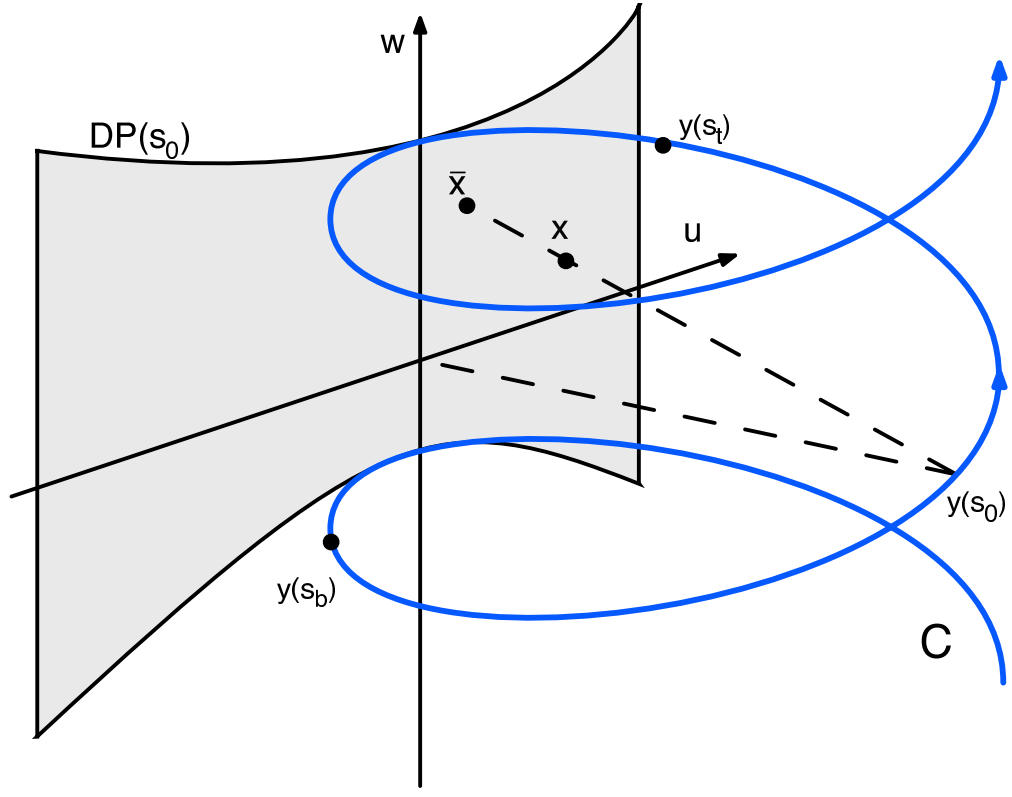

Data: Measurements of the divergent beam transform

$$\mathcal{D}f(\mathbf{y},\boldsymbol{\theta}) = \int_0^\infty f(\mathbf{y}+t\boldsymbol{\theta})\,dt.$$

3D Helical Tomography

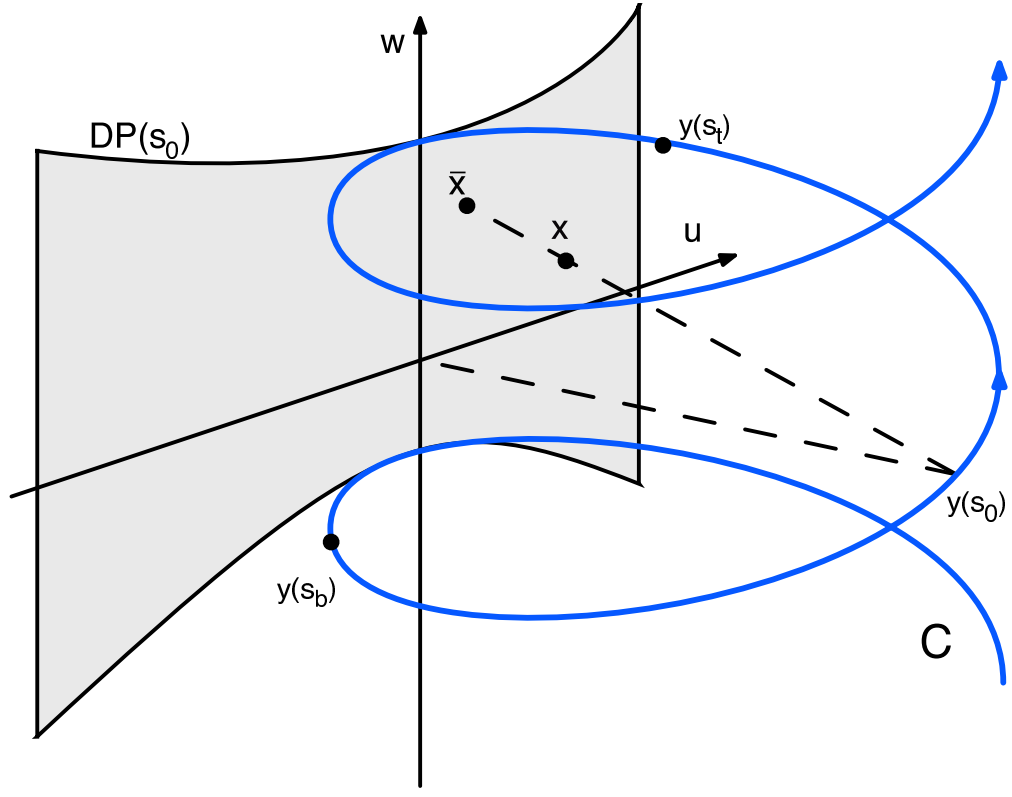

$$\mathcal{D}f(\mathbf{y},\boldsymbol{\theta}) = \int_0^\infty f(\mathbf{y}+t\boldsymbol{\theta})\,dt$$

Integral of f over ray with vertex $\mathbf{y}$ and direction $\boldsymbol{\theta}$.

PI-line and Parametric Interval

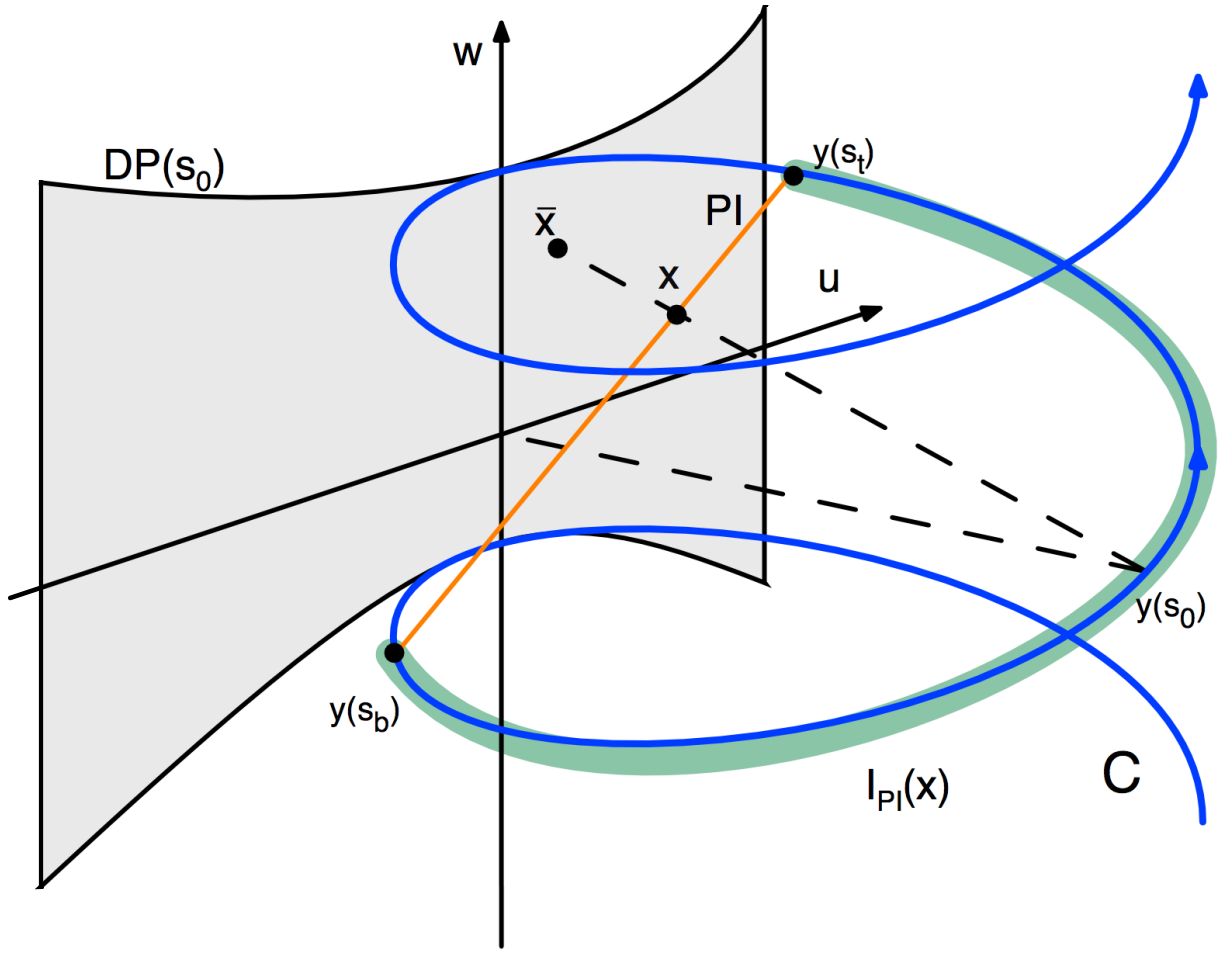

The unique PI-line through $\mathbf{x}$ gives rise to the Parametric Interval $I_{PI}(\mathbf{x}) = [s_b(\mathbf{x}),\ s_t(\mathbf{x})]$

κ-Plane and Katsevich's formula

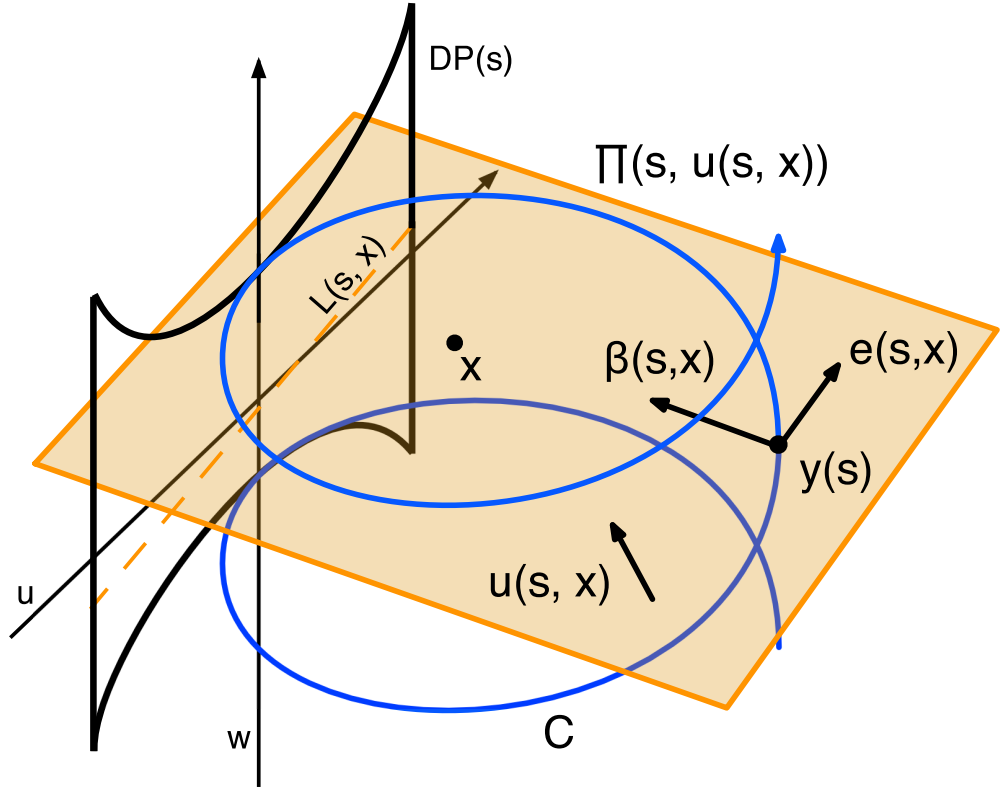

$$\boldsymbol{\beta}(s,\mathbf{x}) = (\mathbf{x}-\mathbf{y}(s))/|\mathbf{x}-\mathbf{y}(s)|$$

κ-Plane and Katsevich's formula

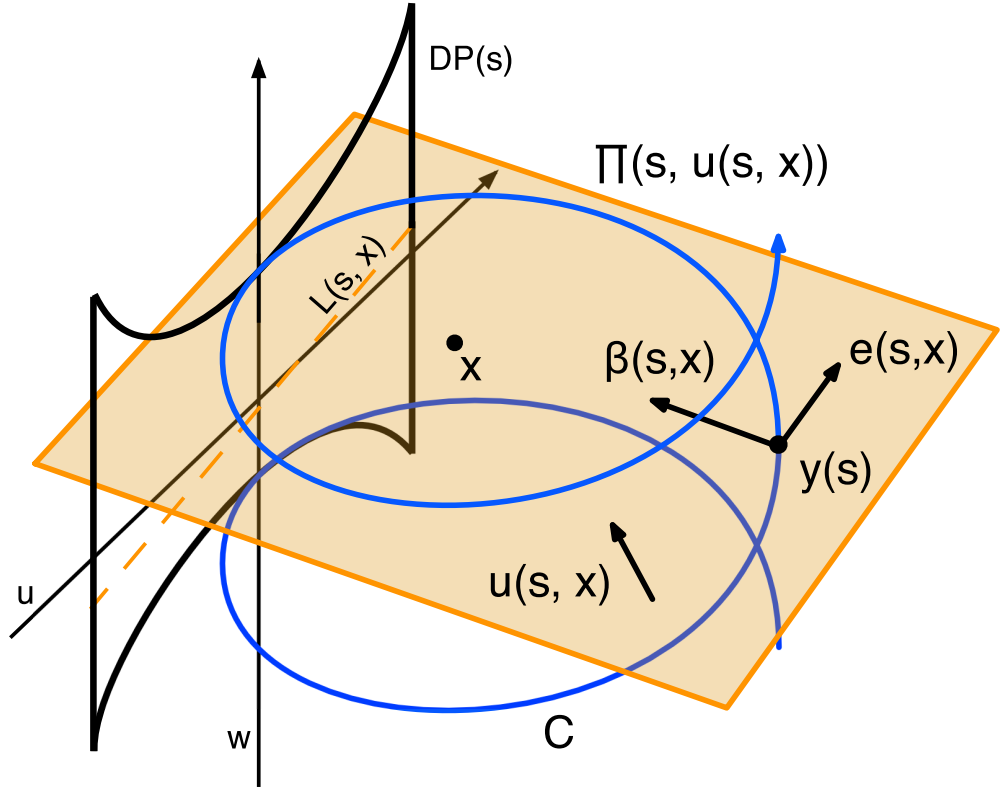

Rays in κ-Plane: $y(s) + t\,\boldsymbol{\Theta}(s, \mathbf{x}, \gamma),\ t \geq 0$

$$\boldsymbol{\Theta}(s, \mathbf{x}, \gamma) = \cos(\gamma)\boldsymbol{\beta}(s, \mathbf{x}) + \sin(\gamma)\mathbf{e}(s, \mathbf{x}).$$

κ-Plane and Katsevich's formula

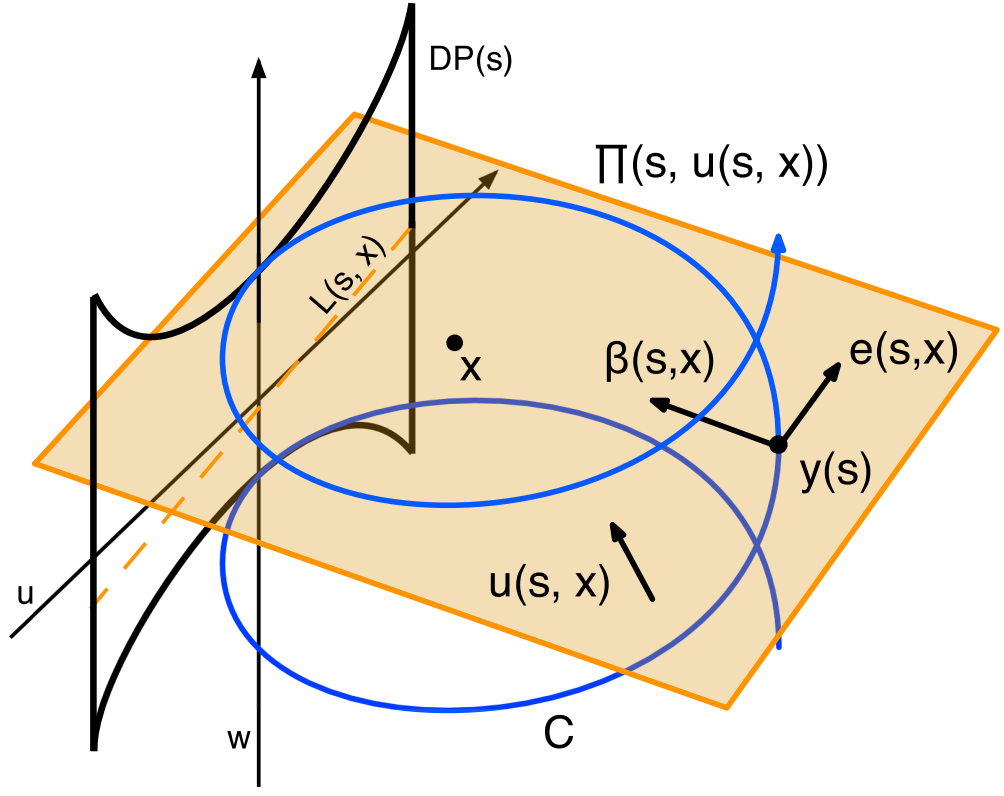

$$f(\mathbf{x}) = \frac{-1}{2\pi^2} \int_{I_{PI}(\mathbf{x})} \frac{1}{|\mathbf{x} - \mathbf{y}(s)|} \int_0^{2\pi} \frac{\partial}{\partial q} \mathcal{D} f(\mathbf{y}(q), \mathbf{\Theta}(s, \mathbf{x}, \gamma))\Big|_{q=s} \frac{d\gamma\, ds}{\sin\gamma}$$

Exploration: Large pitch vs small pitch

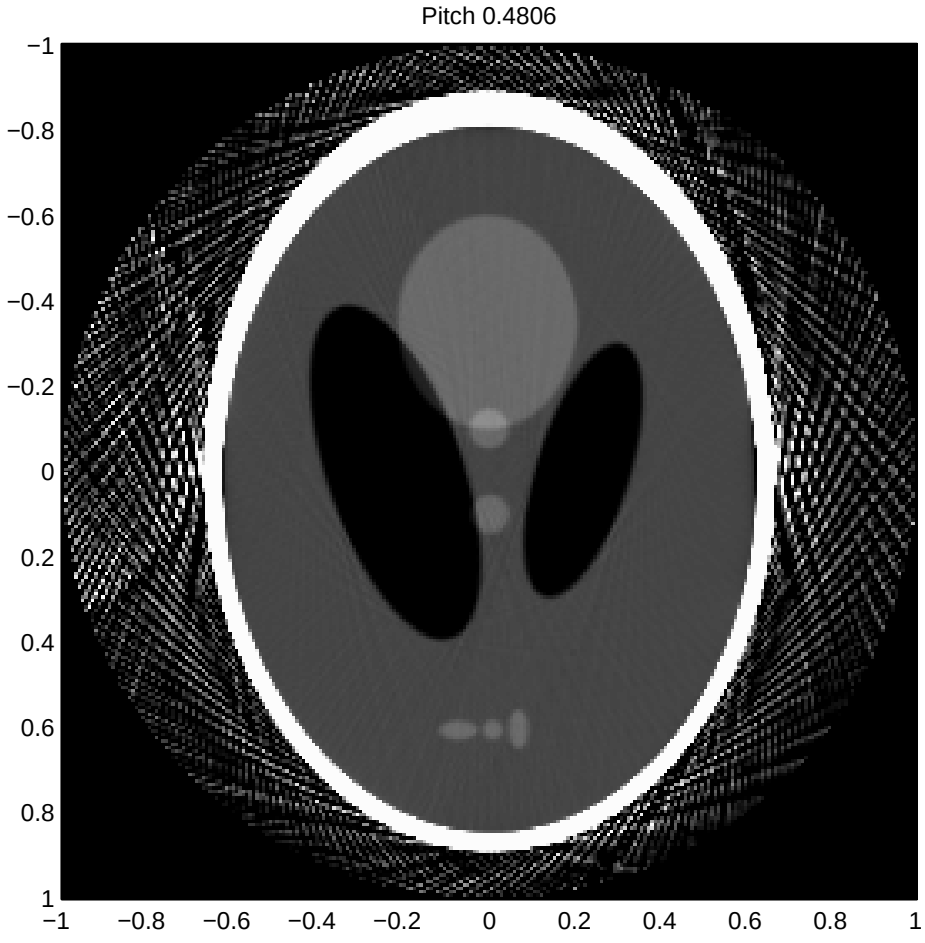

Pitch = 0.4806, detector spacing 0.02, Rel. error = 29.4%

Large pitch vs small pitch II

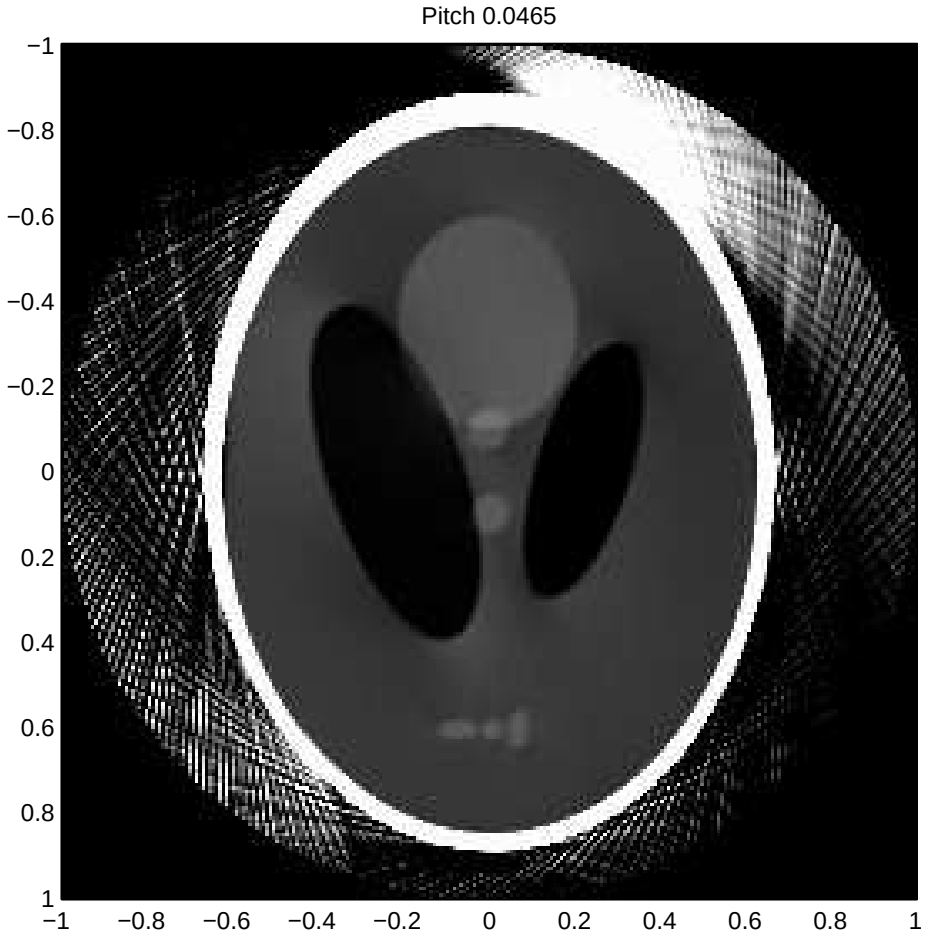

Pitch = 0.0465, detector spacing 0.02, Rel. error = 46.2%.

Limit of vanishing helical pitch

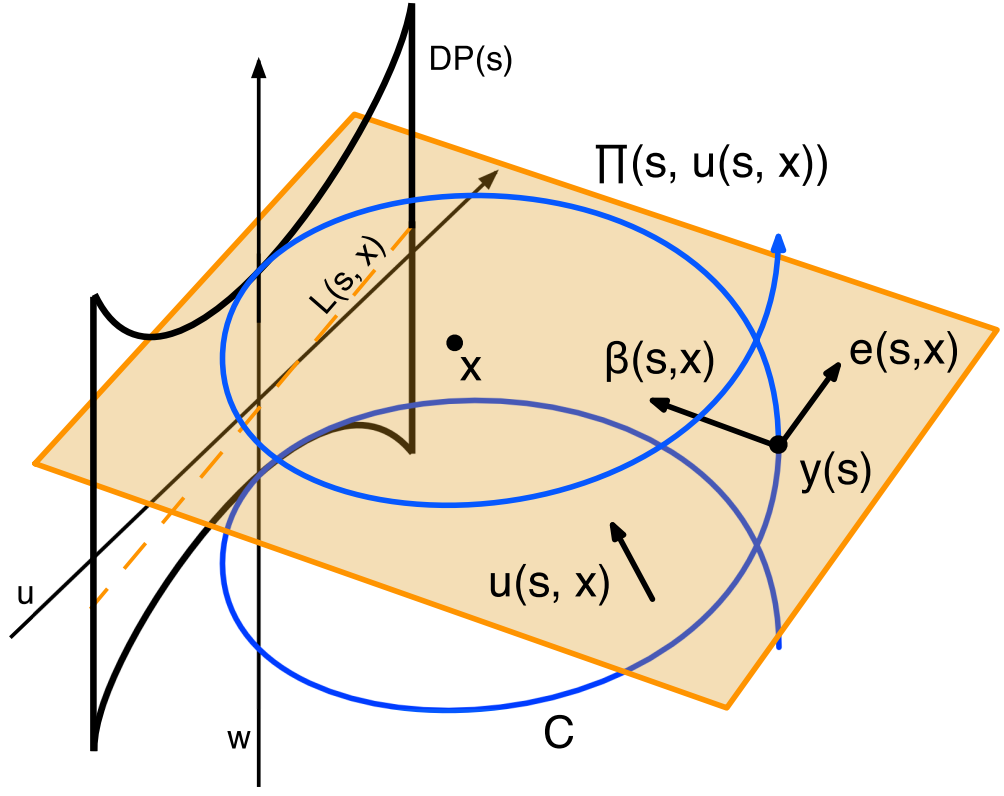

- Let $\mathbf{x} = (x_1, x_2, 0)$. If the pitch P approaches zero the κ-planes become horizontal and the helix shrinks to a circle. Katsevich's formula now gives a 2D fan-beam inversion formula.

Limit of vanishing helical pitch

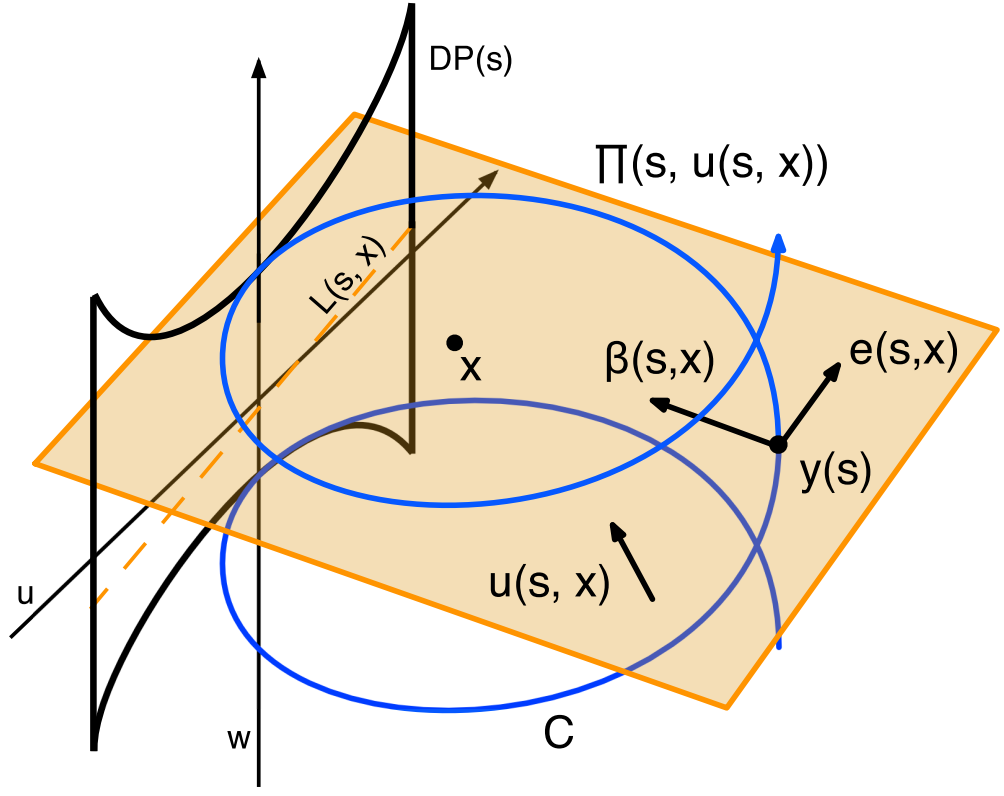

- What is the limit of the PI-lines as $P \to 0$?
  It can be seen from a formula derived by Kyle Champley that in the plane $x_3 = 0$ the interval $I_{PI}(\mathbf{x})$ is independent of the pitch P. So the limit is well-defined.

Limit of vanishing helical pitch

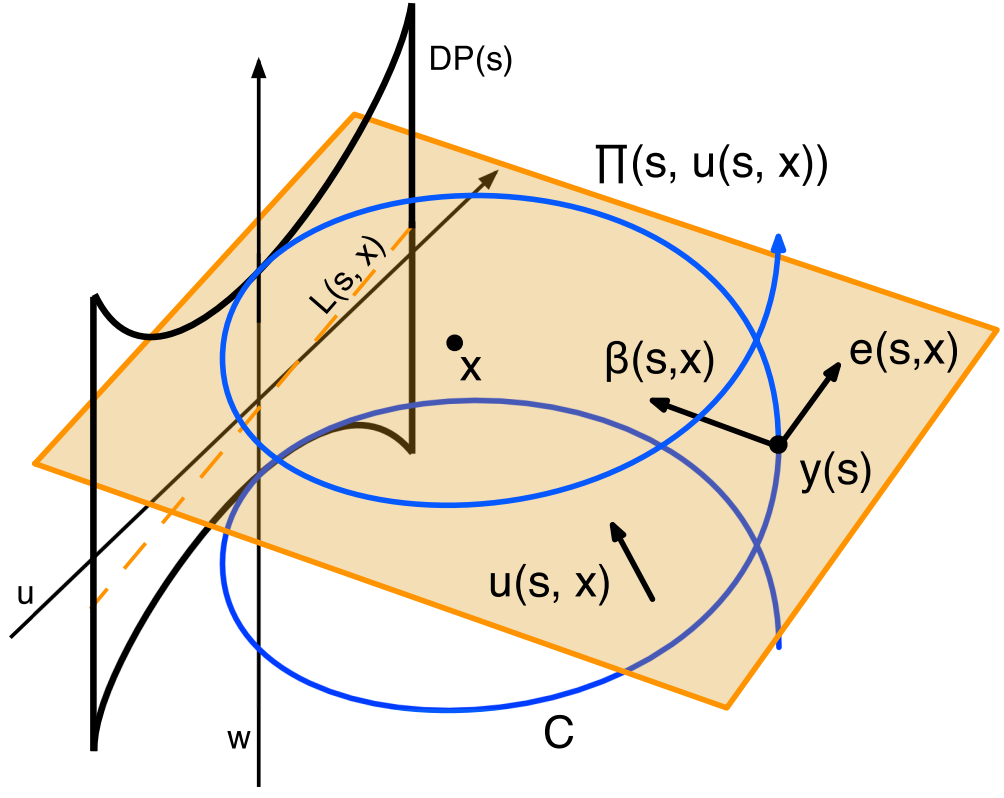

- In fact, the 2D formula is independent of the particular choice of PI-line.

Limit of vanishing helical pitch

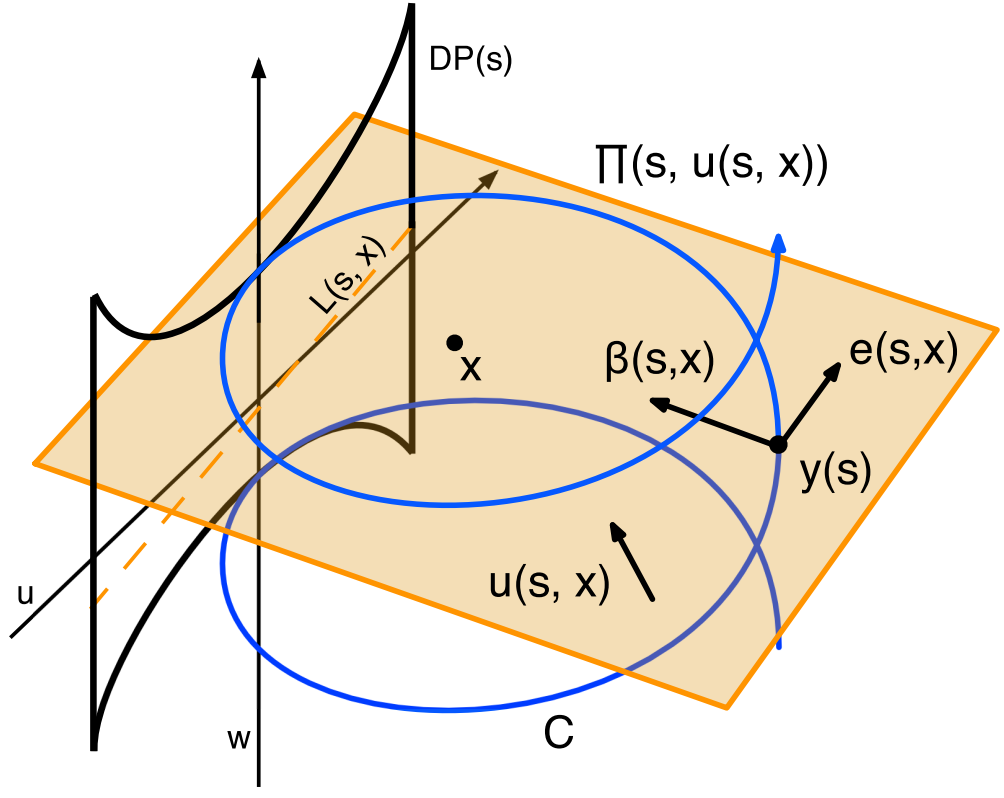

- Related 2D formulas have been derived in the literature; see, e.g., Noo, Defrise, Clackdoyle & Kudo (2002).

Limit $P \to 0$ gives 2D inversion formula

Theorem 1 *Let* $\mathbf{y}(s) = R\,(\cos(s),\, \sin(s))$ *and* $I_{PI}(\mathbf{x})$ *an interval* $s_b \le s \le s_t$ *such that the line segment connecting* $\mathbf{y}(s_b)$ *and* $\mathbf{y}(s_t)$ *contains* $\mathbf{x}$*. Then*

$$f(\mathbf{x}) =$$

$$\frac{-1}{2\pi^2} \int_{I_{PI}(\mathbf{x})} \frac{1}{|\mathbf{x} - \mathbf{y}(s)|} \int_0^{2\pi} \frac{\partial}{\partial q}\, \mathcal{D}f(\mathbf{y}(q),\, \boldsymbol{\Theta}(s, \mathbf{x}, \gamma))|_{q=s}\, \frac{d\gamma\, ds}{\sin\gamma},$$

where $\boldsymbol{\Theta}(s, \mathbf{x}, \gamma) = \cos\gamma\, \boldsymbol{\beta} + \sin\gamma\, \mathbf{e},$

$$\boldsymbol{\beta} = \boldsymbol{\beta}(s, \mathbf{x}) = (\mathbf{x} - \mathbf{y}(s))/|\mathbf{x} - \mathbf{y}(s)|, \quad \mathbf{e} = (-\beta_2,\, \beta_1),$$

Limit $P \to 0$ gives 2D inversion formula

Theorem 2 *Let* $\mathbf{y}(s) = R\,(\cos(s),\, \sin(s))$ *and* $I_{PI}(\mathbf{x})$ *an interval* $s_b \le s \le s_t$ *such that the line segment connecting* $\mathbf{y}(s_b)$ *and* $\mathbf{y}(s_t)$ *contains* $\mathbf{x}$*. Then*

$$f(\mathbf{x}) =$$

$$\frac{-1}{2\pi^2} \int_{I_{PI}(\mathbf{x})} \frac{1}{|\mathbf{x}-\mathbf{y}(s)|} \int_0^{2\pi} \frac{\partial}{\partial q}\, \mathcal{D}f(\mathbf{y}(q),\, \boldsymbol{\Theta}(s,\mathbf{x},\gamma))|_{q=s}\, \frac{d\gamma\, ds}{\sin\gamma},$$

where $\boldsymbol{\Theta}(s,\mathbf{x},\gamma) = \cos\gamma\, \boldsymbol{\beta} + \sin\gamma\, \mathbf{e},$

$$\boldsymbol{\beta} = \boldsymbol{\beta}(s,\mathbf{x}) = (\mathbf{x}-\mathbf{y}(s))/|\mathbf{x}-\mathbf{y}(s)|, \quad \mathbf{e} = (-\beta_2,\, \beta_1),$$

- Remark: $\mathbf{y}(s)$ does not need to be a circle!

2D fan-beam coordinates

$$y(s) = R(\cos(s), \sin(s)), \quad \boldsymbol{\theta} = -(\cos(s-\alpha),\, \sin(s-\alpha))$$

$$Df(\mathbf{y}, \boldsymbol{\theta}) = g(s, \alpha).$$

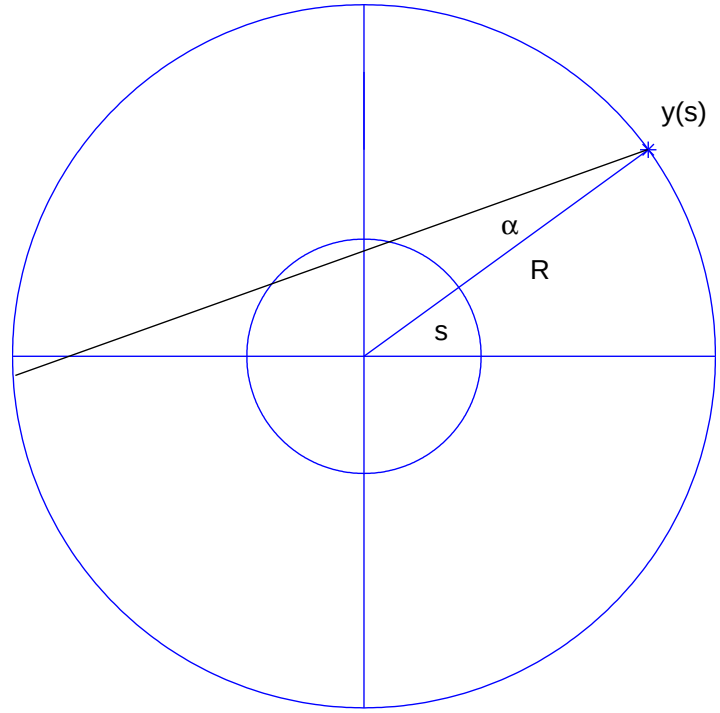

2D formula in fan-beam coordinates

$$f(\mathbf{x})$$

$$= \frac{-1}{2\pi^2} \int_{I_{PI}(\mathbf{x})} \frac{1}{|\mathbf{x}-\mathbf{y}(s)|} \int_0^{2\pi} \frac{\partial}{\partial q} \mathcal{D}f(\mathbf{y}(q),\, \mathbf{\Theta}(s,\mathbf{x},\gamma))|_{q=s} \; \frac{d\gamma\, ds}{\sin\gamma},$$

$$= \frac{1}{2\pi^2} \int_{I_{PI}(x)} \frac{1}{|\mathbf{x}-\mathbf{y}(s)|} \int_0^{2\pi} \left(\frac{\partial g}{\partial s} + \frac{\partial g}{\partial \alpha}\right) \; \frac{d\alpha\, ds}{\sin(\alpha^* - \alpha)}$$

The value $\alpha = \alpha^*$ corresponds to the ray from $\mathbf{y}(s)$ through $\mathbf{x}$.

Relationship to other 2D formulas

Consider the 2D x-ray transform.

$$\mathcal{P}f(\varphi, p) = \int f(p\boldsymbol{\omega}^{\perp} + t\boldsymbol{\omega})\, dt.$$

$$\boldsymbol{\omega} = (\cos\varphi,\ \sin\varphi), \quad \boldsymbol{\omega}^{\perp} = (-\sin\varphi,\ \cos\varphi).$$

$\mathcal{P}f$ and $g(s, \alpha)$ are related via a change of variables.

$$g(s, \alpha) \ = \ \mathcal{P}f(s - \alpha,\ R\sin\alpha)$$

Fan-beam formula via change of variables

Classical Radon inversion formula (parallel-beam)

$$f(x) = \frac{1}{4\pi^2} \int_0^{2\pi} \int \frac{\partial \mathcal{P} f(\varphi, p)}{\partial p} \frac{dp}{\langle \mathbf{x}, \boldsymbol{\omega}^{\perp} \rangle - p} \, d\varphi.$$

Fan-beam formula via change of variables

Classical Radon inversion formula (parallel-beam)

$$f(x) = \frac{1}{4\pi^2} \int_0^{2\pi} \int \frac{\partial \mathcal{P} f(\varphi, p)}{\partial p} \frac{dp}{\langle \mathbf{x}, \boldsymbol{\omega}^{\perp} \rangle - p} \, d\varphi.$$

Changing variables in Radon's inversion formula for the 2D x-ray transform gives

$$f(x) = \frac{1}{4\pi^2} \int_0^{2\pi} \frac{1}{|\mathbf{x} - \mathbf{y}(s)|} \int_0^{2\pi} \left(\frac{\partial g}{\partial s} + \frac{\partial g}{\partial \alpha} \right) \frac{d\alpha \, ds}{\sin(\alpha^* - \alpha)}.$$

(Herman and Naparstek (1977))

Comparison.

Herman and Naparstek's formula:

$$f(x) \;=\; \frac{1}{4\pi^2}\int_0^{2\pi}\frac{1}{|\mathbf{x}-\mathbf{y}(s)|}\int_0^{2\pi}\left(\frac{\partial g}{\partial s}+\frac{\partial g}{\partial \alpha}\right)\,\frac{d\alpha\,ds}{\sin(\alpha^*-\alpha)}.$$

Comparison.

Herman and Naparstek's formula:

$$f(x) \;=\; \frac{1}{4\pi^2}\int_0^{2\pi}\frac{1}{|\mathbf{x}-\mathbf{y}(s)|}\int_0^{2\pi}\left(\frac{\partial g}{\partial s}+\frac{\partial g}{\partial \alpha}\right)\frac{d\alpha\,ds}{\sin(\alpha^*-\alpha)}.$$

Katsevich's 2D formula in fan-beam coordinates.

$$f(x) \;=\; \frac{1}{2\pi^2}\int_{I_{PI}(x)}\frac{1}{|\mathbf{x}-\mathbf{y}(s)|}\int_0^{2\pi}\left(\frac{\partial g}{\partial s}+\frac{\partial g}{\partial \alpha}\right)\frac{d\alpha\,ds}{\sin(\alpha^*-\alpha)}$$

Comparison.

Herman and Naparstek's formula:

$$f(x) \;=\; \frac{1}{4\pi^2}\int_0^{2\pi}\frac{1}{|\mathbf{x}-\mathbf{y}(s)|}\int_0^{2\pi}\left(\frac{\partial g}{\partial s}+\frac{\partial g}{\partial \alpha}\right)\frac{d\alpha\, ds}{\sin(\alpha^*-\alpha)}.$$

Katsevich's 2D formula in fan-beam coordinates.

$$f(x) \;=\; \frac{1}{2\pi^2}\int_{I_{PI}(x)}\frac{1}{|\mathbf{x}-\mathbf{y}(s)|}\int_0^{2\pi}\left(\frac{\partial g}{\partial s}+\frac{\partial g}{\partial \alpha}\right)\frac{d\alpha\, ds}{\sin(\alpha^*-\alpha)}$$

- Difference: Interval of integration with respect to s.

Comparison.

Herman and Naparstek's formula:

$$f(x) \;=\; \frac{1}{4\pi^2}\int_0^{2\pi}\frac{1}{|\mathbf{x}-\mathbf{y}(s)|}\int_0^{2\pi}\left(\frac{\partial g}{\partial s}+\frac{\partial g}{\partial \alpha}\right)\frac{d\alpha\,ds}{\sin(\alpha^*-\alpha)}.$$

Katsevich's 2D formula in fan-beam coordinates.

$$f(x) \;=\; \frac{1}{2\pi^2}\int_{I_{PI}(x)}\frac{1}{|\mathbf{x}-\mathbf{y}(s)|}\int_0^{2\pi}\left(\frac{\partial g}{\partial s}+\frac{\partial g}{\partial \alpha}\right)\frac{d\alpha\,ds}{\sin(\alpha^*-\alpha)}$$

- Difference: Interval of integration with respect to s.
- $I_{PI}(\mathbf{x})$ decomposes the circle into two arcs. Averaging Katsevich's formula over these two complementary arcs gives Herman and Naparstek's formula.

Summary

$$f(\mathbf{x}) = \frac{-1}{2\pi^2} \int_{I_{PI}(\mathbf{x})} \frac{1}{|\mathbf{x} - \mathbf{y}(s)|} \int_0^{2\pi} \frac{\partial}{\partial q} \mathcal{D} f(\mathbf{y}(q), \mathbf{\Theta}(s, \mathbf{x}, \gamma))\Big|_{q=s} \frac{d\gamma\, ds}{\sin\gamma}$$

Summary

$$f(\mathbf{x}) = \frac{-1}{2\pi^2} \int_{I_{PI}(\mathbf{x})} \frac{1}{|\mathbf{x} - \mathbf{y}(s)|} \int_0^{2\pi} \frac{\partial}{\partial q} \mathcal{D} f(\mathbf{y}(q), \mathbf{\Theta}(s, \mathbf{x}, \gamma))\Big|_{q=s} \frac{d\gamma\, ds}{\sin\gamma}$$

- Katsevich's formula holds both in 2D and 3D.

Summary

$$f(\mathbf{x}) = \frac{-1}{2\pi^2} \int_{I_{PI}(\mathbf{x})} \frac{1}{|\mathbf{x} - \mathbf{y}(s)|} \int_0^{2\pi} \frac{\partial}{\partial q} \mathcal{D} f(\mathbf{y}(q), \mathbf{\Theta}(s, \mathbf{x}, \gamma))\Big|_{q=s} \frac{d\gamma\, ds}{\sin\gamma}$$

- Katsevich's formula holds both in 2D and 3D.
- Source curves are not restricted to be a circle in 2D or a helix in 3D (Katsevich & Kapralov (2007)).

Summary

$$f(\mathbf{x}) = \frac{-1}{2\pi^2} \int_{I_{PI}(\mathbf{x})} \frac{1}{|\mathbf{x} - \mathbf{y}(s)|} \int_0^{2\pi} \frac{\partial}{\partial q} \mathcal{D} f(\mathbf{y}(q), \mathbf{\Theta}(s, \mathbf{x}, \gamma))\Big|_{q=s} \frac{d\gamma\, ds}{\sin\gamma}$$

- Katsevich's formula holds both in 2D and 3D.
- Source curves are not restricted to be a circle in 2D or a helix in 3D (Katsevich & Kapralov (2007)).
- It is a fundamental formula in tomography.

Summary, cont.

$$f(\mathbf{x}) = \frac{-1}{2\pi^2} \int_{I_{PI}(\mathbf{x})} \frac{1}{|\mathbf{x} - \mathbf{y}(s)|} \int_0^{2\pi} \frac{\partial}{\partial q} \mathcal{D} f(\mathbf{y}(q), \mathbf{\Theta}(s, \mathbf{x}, \gamma))\Big|_{q=s} \frac{d\gamma\, ds}{\sin\gamma}$$

- In 2D, Katsevich's formula uses fewer line integrals than Radon's formula. It cannot be obtained by a change of variables.

Summary, cont.

$$f(\mathbf{x}) = \frac{-1}{2\pi^2} \int_{I_{PI}(\mathbf{x})} \frac{1}{|\mathbf{x}-\mathbf{y}(s)|} \int_0^{2\pi} \frac{\partial}{\partial q} \mathcal{D}f(\mathbf{y}(q), \boldsymbol{\Theta}(s,\mathbf{x},\gamma))\Big|_{q=s} \frac{d\gamma\, ds}{\sin\gamma}$$

- In 2D, Katsevich's formula uses fewer line integrals than Radon's formula. It cannot be obtained by a change of variables.
- The deeper relation

$$\int_{S^1} \mathcal{D}f(\mathbf{y}(s), \boldsymbol{\theta}) \frac{d\boldsymbol{\theta}}{\boldsymbol{\theta}\cdot\boldsymbol{\omega}^\perp} = \int \mathcal{P}f(\varphi, p) \frac{dp}{p - \mathbf{y}(s)\cdot\boldsymbol{\omega}^\perp}$$

  is required. Originally due to Hamaker, Smith, Solmon and Wagner (1980). Its usefulness in 3D was pointed out by Natterer (1994).

Numerical exploration of H.-N. formula

$$f(x) = \frac{1}{4\pi^2} \int_0^{2\pi} \frac{1}{|\mathbf{x} - \mathbf{y}(s)|} \int_0^{2\pi} \left(\frac{\partial g}{\partial s} + \frac{\partial g}{\partial \alpha} \right) \frac{d\alpha \, ds}{\sin(\alpha^* - \alpha)}.$$

Motivation.

- Shares some features with 3D formula and allows to study these separately.
- Standard 2D fan-beam FBP algorithm does not have optimal resolution (Kruse (1989), F. (2006), Izen (2007)). Perhaps this formula leads to a better algorithm ??
- Sampling theory for 2D fan-beam is well understood (Natterer(1993), Palamodov(1995), F. (2006)).

Implementation of convolution

For numerical implementation of the convolution with $1/\sin(\alpha)$ write

$$\frac{1}{\sin\alpha} = \frac{1}{\alpha}\,\frac{\alpha}{\sin\alpha}$$

and then regularize the Hilbert transform kernel $1/\alpha$, similar to 2D fan-beam tomography (cf. Herman & Naparstek (1977)).

Implementation of convolution

For numerical implementation of the convolution with $1/\sin(\alpha)$ write

$$\frac{1}{\sin\alpha} = \frac{1}{\alpha}\,\frac{\alpha}{\sin\alpha}$$

and then regularize the Hilbert transform kernel $1/\alpha$, similar to 2D fan-beam tomography (cf. Herman & Naparstek (1977)). We obtain

$$\int_0^{2\pi}\left(\frac{\partial g}{\partial s}+\frac{\partial g}{\partial \alpha}\right)\,\frac{d\alpha}{\sin(\alpha^*-\alpha)} \simeq \int_0^{2\pi}\left(\frac{\partial g}{\partial s}+\frac{\partial g}{\partial \alpha}\right)\,k(\alpha^*-\alpha)d\alpha$$

with

$$k(\alpha) = i\,\frac{1-\cos(b\alpha)}{\alpha}\frac{\alpha}{\sin\alpha} = i\,\frac{1-\cos(\alpha)}{\sin\alpha}.$$

Implementation of derivatives I

Use, e.g., central differences for the derivatives. E.g.,

$$\frac{\partial g}{\partial s} \simeq \frac{1}{2\Delta s}\left(g(s_{j+1},\alpha_l) - g(s_{j-1},\alpha_l)\right),$$

and similarly for $\partial g/\partial\alpha$. This approximates the derivatives at (s_j,α_l). (Labeled M1 in images to follow).

Implementation of derivatives II

Or approximate derivatives at $(s_{j+1/2}, \alpha_{l+1/2})$ via

$$\frac{\partial g}{\partial s} \simeq \frac{1}{2\Delta s}\left[(g(s_{j+1},\alpha_l) - g(s_j,\alpha_l))\right.$$

$$\left. + \ (g(s_{j+1},\alpha_{l+1}) - g(s_j,\alpha_{l+1}))\right]$$

In this case there are two natural choices for implementing the convolution and backprojection.

- Use unshifted discrete convolution kernel and incorporate shift in backprojection step. (Labeled M2 in images to follow).
- Incorporate shift in the discrete convolution kernel. (Labeled M3 in images to follow).

Standard 2D fan-beam algorithm.

$$f(\mathbf{x}) = \lim_{c\to\infty} f_c(x) =$$

$$\lim_{c\to\infty} R \int_0^{2\pi} \int_0^{2\pi} k_c(\alpha^* - \alpha) \left(\frac{\alpha^* - \alpha}{\sin(\alpha^* - \alpha)} \right)^2 g(s, \alpha) \cos\alpha \; d\alpha \; ds$$

Standard 2D fan-beam algorithm.

$$f(\mathbf{x}) = \lim_{c\to\infty} f_c(x) =$$

$$\lim_{c\to\infty} R \int_0^{2\pi} \int_0^{2\pi} k_c(\alpha^* - \alpha) \left(\frac{\alpha^* - \alpha}{\sin(\alpha^* - \alpha)} \right)^2 g(s, \alpha) \cos\alpha \; d\alpha \; ds$$

- $k_c(t) = \frac{1}{8\pi^2} \int_{-c}^{c} |\sigma| e^{i\sigma t} \, d\sigma$ "ramp filter"

Standard 2D fan-beam algorithm.

$$f(\mathbf{x}) = \lim_{c\to\infty} f_c(x) =$$

$$\lim_{c\to\infty} R \int_0^{2\pi} \int_0^{2\pi} k_c(\alpha^* - \alpha) \left(\frac{\alpha^* - \alpha}{\sin(\alpha^* - \alpha)} \right)^2 g(s, \alpha) \cos\alpha \; d\alpha \; ds$$

- $k_c(t) = \frac{1}{8\pi^2} \int_{-c}^{c} |\sigma| e^{i\sigma t} \, d\sigma$ "ramp filter"
- No derivative with respect to s.

Standard 2D fan-beam algorithm.

$$f(\mathbf{x}) = \lim_{c\to\infty} f_c(x) =$$

$$\lim_{c\to\infty} R \int_0^{2\pi}\int_0^{2\pi} k_c(\alpha^* - \alpha)\left(\frac{\alpha^* - \alpha}{\sin(\alpha^* - \alpha)}\right)^2 g(s,\alpha)\cos\alpha\, d\alpha\, ds$$

- $k_c(t) = \frac{1}{8\pi^2}\int_{-c}^{c} |\sigma| e^{i\sigma t}\, d\sigma$ "ramp filter"
- No derivative with respect to s.
- Labeled Std. in images to follow.

Experiment with Shepp Logan phantom.

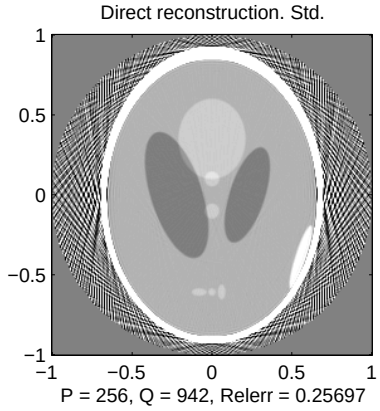

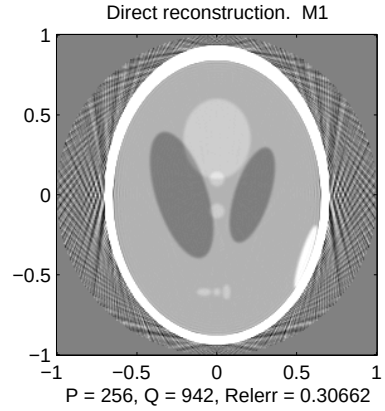

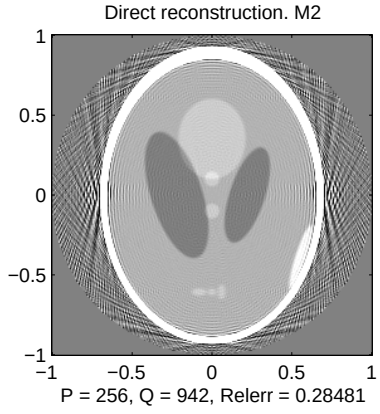

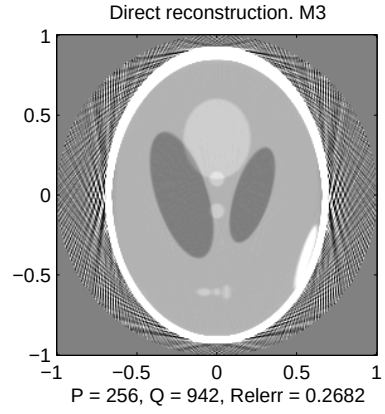

Implementation M2 shows some high-frequency artifacts that M3 does not. Why?

Fourier transform of conv. kernel for M2.

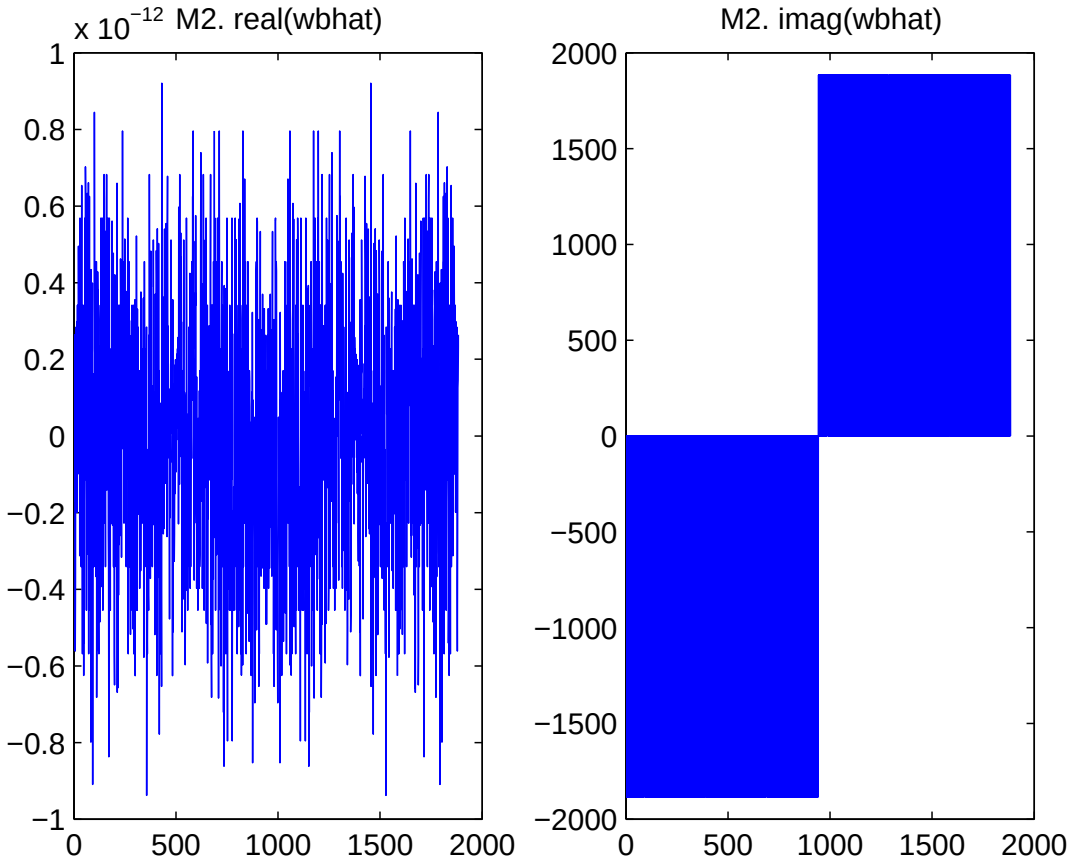

Discontinuity at cut-off frequency.

Fourier transform of conv. kernel for M3.

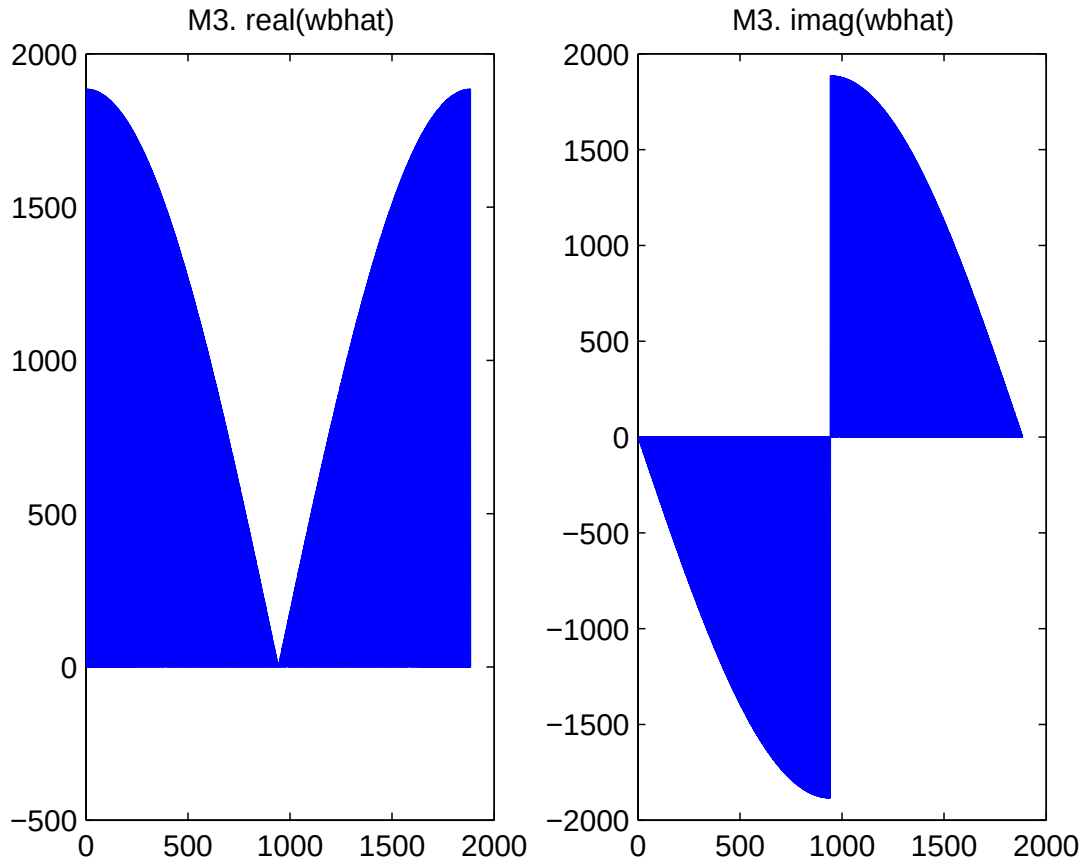

Discontinuity at cut-off frequency is removed for correct sampling.

Experiments with bandlimited phantom

$$f(\mathbf{x}) = \frac{J_1(b|\mathbf{x}-\mathbf{x}_0|)}{b|\mathbf{x}-\mathbf{x}_0|}, \quad b = 100, \quad \mathbf{x}_0 = (0.4, 0.7)$$

$$|\hat{f}(\boldsymbol{\xi})| = \begin{cases} 1/b^2 & \text{if } |\boldsymbol{\xi}| \leq b \\ 0 & \text{otherwise} \end{cases}$$

For $R = 3$ sampling theory yields that $P = 175$ sources and $Q = 300$ rays distributed over $|\alpha| \leq \pi/2$ should suffice for an accurate reconstruction.

Translates of support of $\hat{g}$.

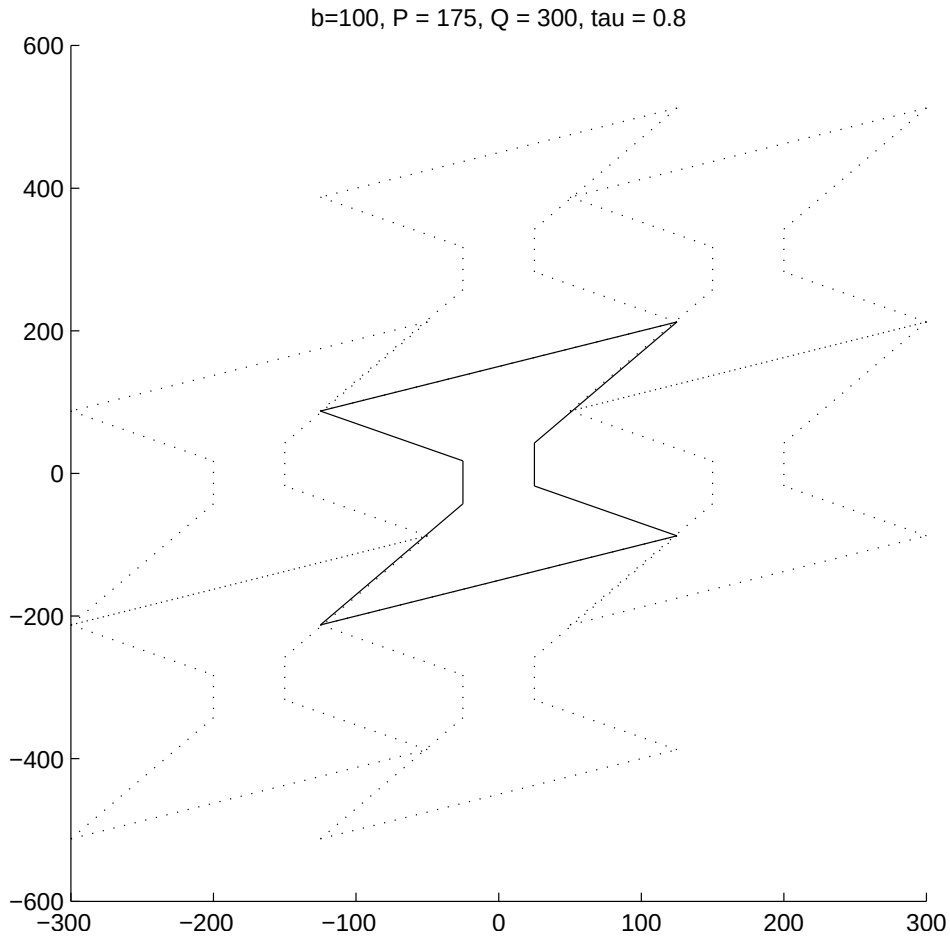

Direct reconstruction.

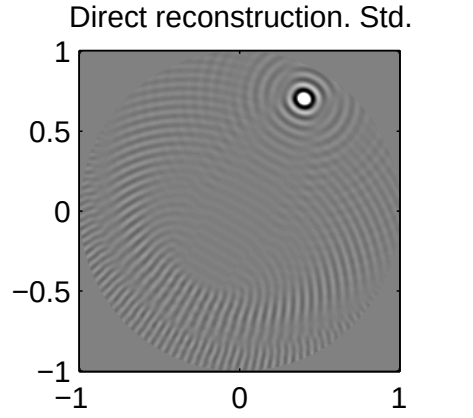

P = 175, Q = 300, Relerr = 0.38367

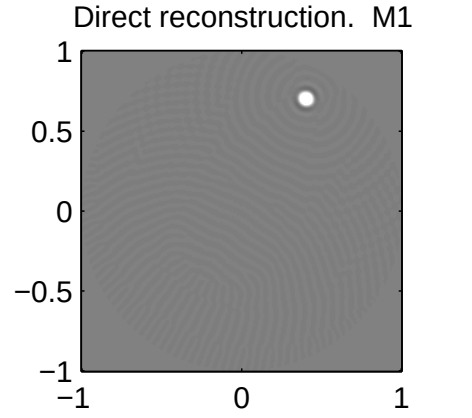

P = 175, Q = 300, Relerr = 0.65592

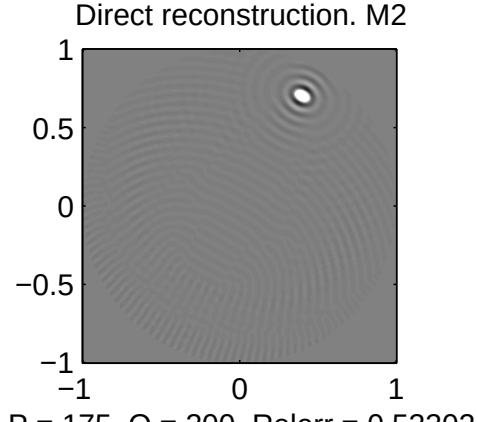

P = 175, Q = 300, Relerr = 0.53302

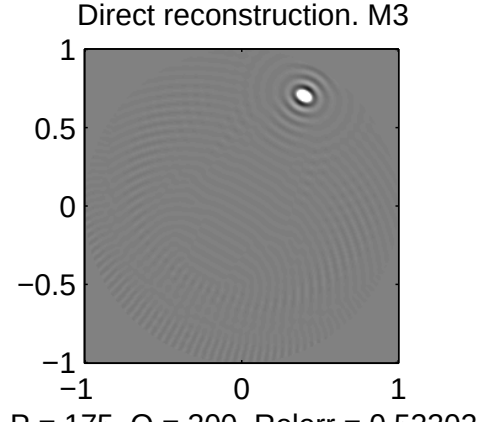

P = 175, Q = 300, Relerr = 0.53302

Interpolated reconstruction.

Use sampling theorem to interpolate data to denser lattice prior to reconstruction.

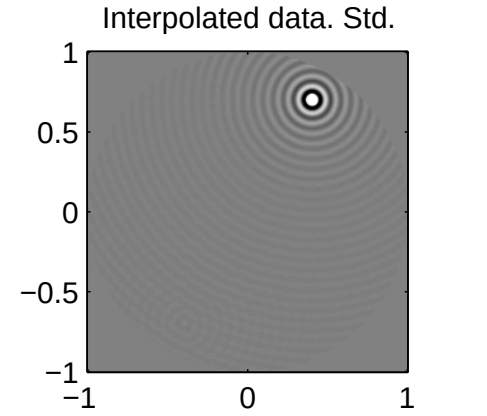

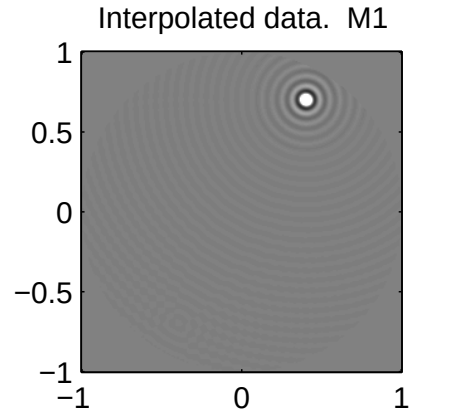

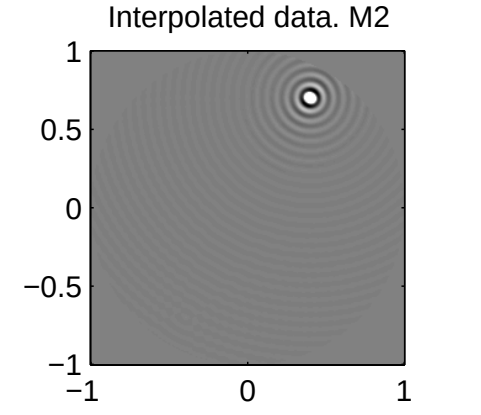

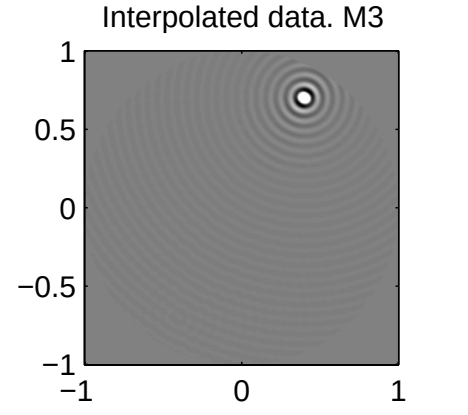

Interpolated reconstruction, $b = 10$.

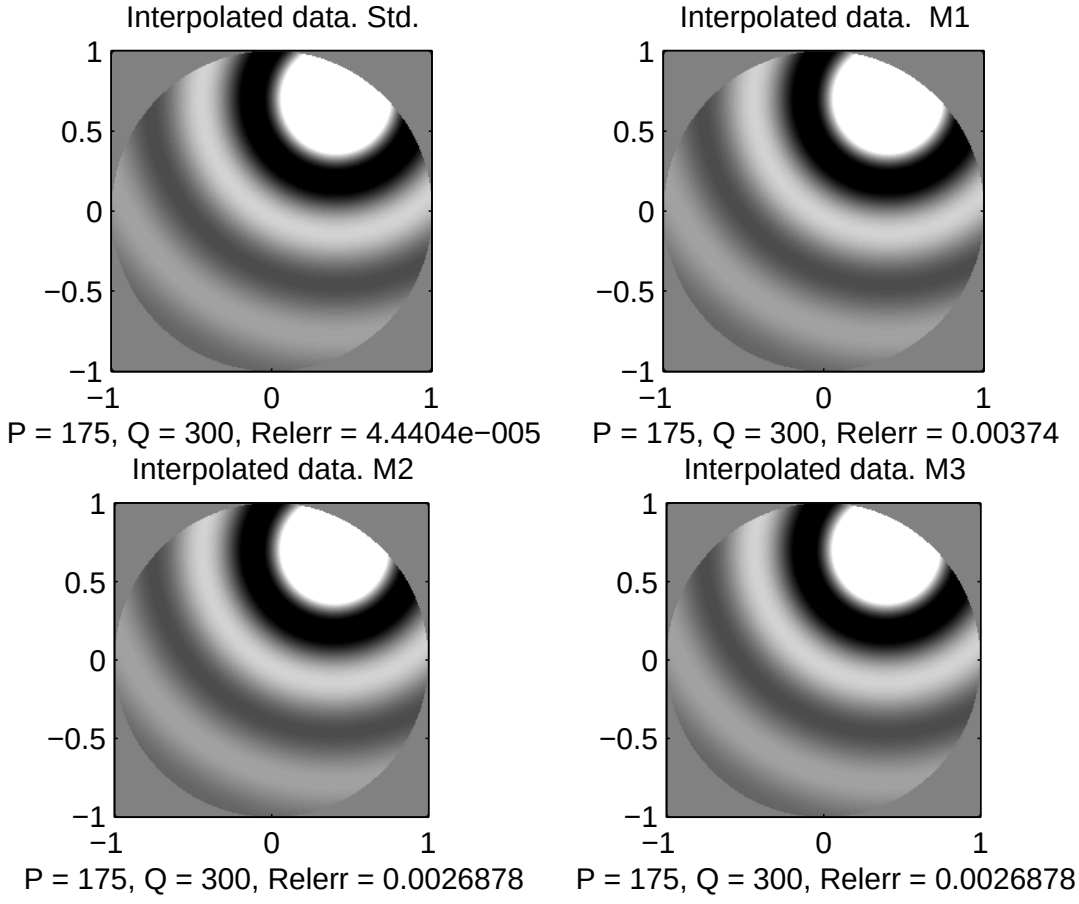

Note that for the bandlimited phantom M2 and M3 give identical results up to round-off.

Drawback of M2 and M3.

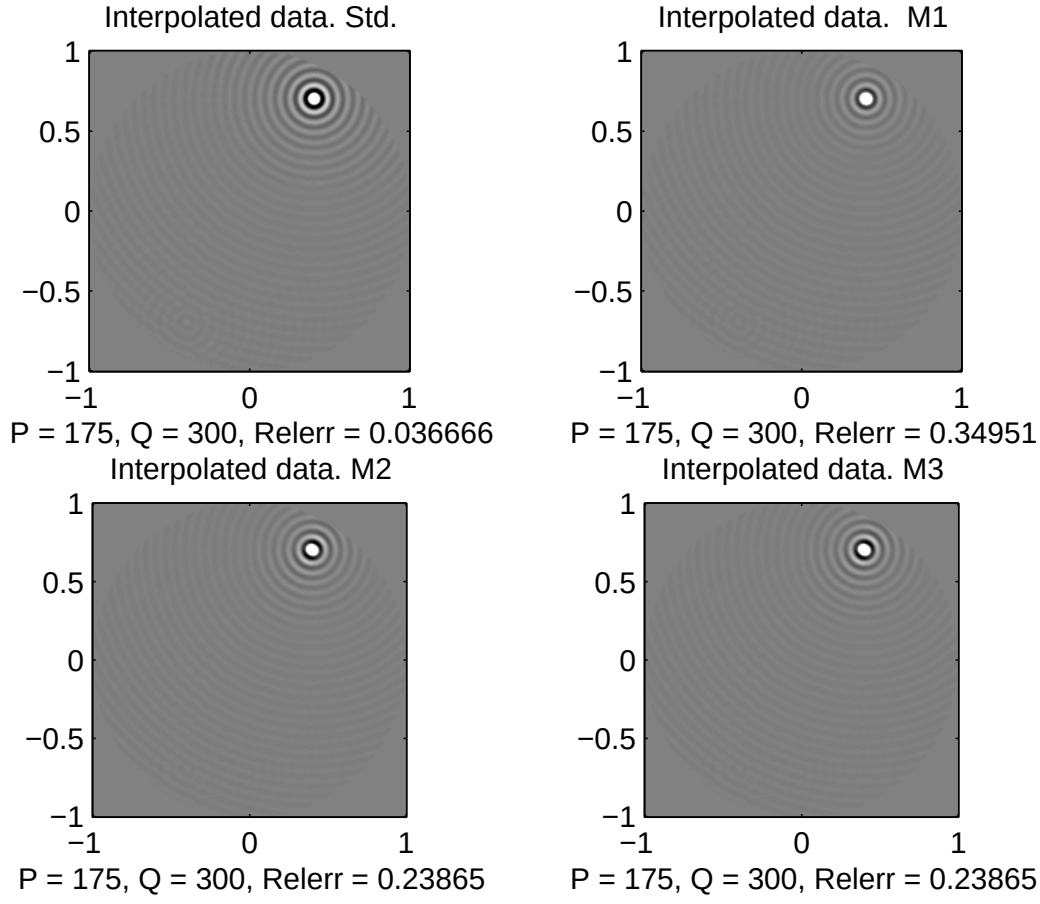

Concern: Peak in M2 and M3 seems to be slightly distorted.

Drawback of M2 and M3, cont.

Indeed, discretizing $\partial g/\partial \alpha$ (which is usually much larger than $\partial g/\partial s$)as

$$\frac{\partial g}{\partial \alpha}(s_{j+1/2}, \alpha_{l+1/2}) \simeq \frac{1}{2\Delta\alpha}\,[g(s_j, \alpha_{l+1}) - g(s_j, \alpha_l) + g(s_{j+1}, \alpha_{l+1}) - g(s_{j+1}, \alpha_l)]$$

can be viewed as averaging over two slightly rotated images.

Drawback of M2 and M3, cont.

Better: Use only first term and compute derivatives at $(s_j, \alpha_{j+1/2})$. Can use larger stepsize for $\partial g/\partial s$ to get correct alignment (M4).

$$\frac{\partial g}{\partial \alpha}(s_j, \alpha_{l+1/2}) \simeq \frac{1}{\Delta\alpha}\left[g(s_j, \alpha_{l+1}) - g(s_j, \alpha_l)\right]$$

$$\frac{\partial g}{\partial s}(s_j, \alpha_{l+1/2}) \simeq \frac{1}{4\Delta s}\left[(g(s_{j+1}, \alpha_l) - g(s_{j-1}, \alpha_l)) + (g(s_{j+1}, \alpha_{l+1}) - g(s_{j-1}, \alpha_{l+1}))\right]$$

This is method M4.

Method M4

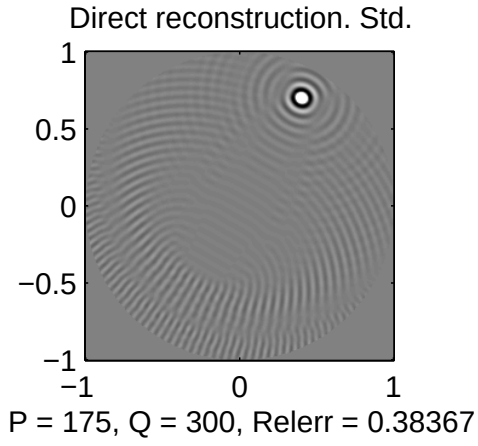
Direct reconstruction. Std.
1
0.5
0
−0.5
−1
−1
0
1
P = 175, Q = 300, Relerr = 0.38367

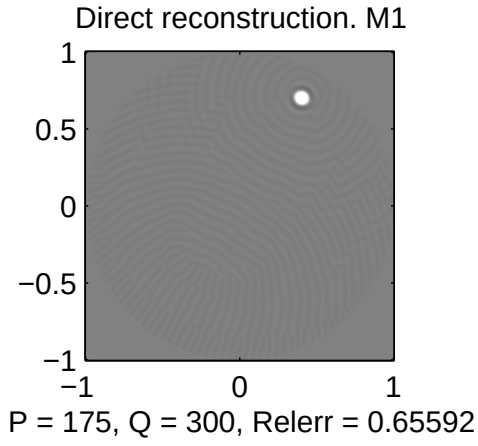
Direct reconstruction. M1
1
0.5
0
−0.5
−1
−1
0
1
P = 175, Q = 300, Relerr = 0.65592

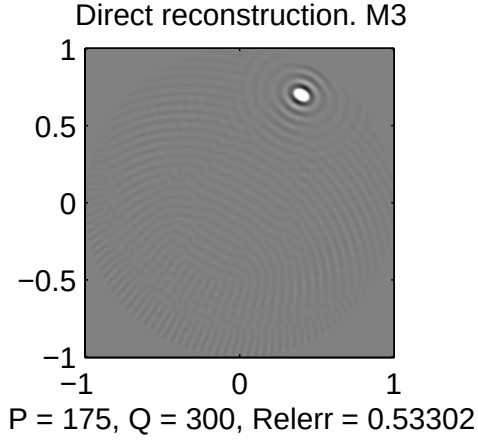
Direct reconstruction. M3
1
0.5
0
−0.5
−1
−1
0
1
P = 175, Q = 300, Relerr = 0.53302

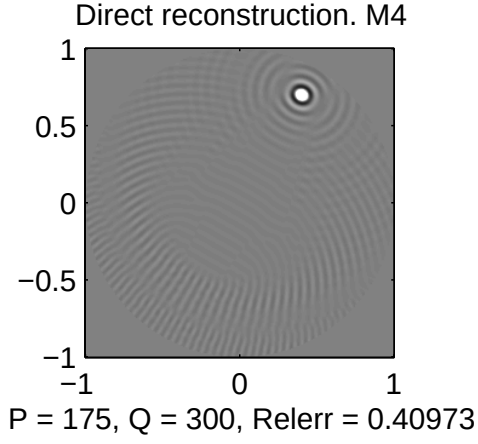
Direct reconstruction. M4
1
0.5
0
−0.5
−1
−1
0
1
P = 175, Q = 300, Relerr = 0.40973

Conclusions

- Shift in convolution kernel helps to remove some artifacts but does not increase resolution.

Conclusions

- Shift in convolution kernel helps to remove some artifacts but does not increase resolution.
- It is hard to beat the standard algorithm, but method M4 is almost as good, with some room left for possible improvements.

Conclusions

- Shift in convolution kernel helps to remove some artifacts but does not increase resolution.
- It is hard to beat the standard algorithm, but method M4 is almost as good, with some room left for possible improvements.
- Preprint available on Adel Faridani's webpage.